Science and Technology Indonesia
e-ISSN:2580-4391 *p*-ISSN:2580-4405
Vol. 10, No. 1, January 2025

Research Paper

Fluorine Substitution in Diamine Covalent Organic Frameworks: Computational Analysis of CO_2/N_2 Adsorption and Permeability

Noviyan Darmawan[1*], Yusuf Bramastya Apriliyanto[2], Andreas Ary Chrisna Jati[1], Cahyorini Kusumawardani[3]

[1]*Department of Chemistry, IPB University, Bogor, 16680, Indonesia*
[2]*Department of Chemistry, The Republic of Indonesia Defense University, Bogor, 16810, Indonesia*
[3]*Department of Chemistry, Yogyakarta State University, Yogyakarta, 55281, Indonesia*
***Corresponding author**: noviyandarmawan@apps.ipb.ac.id

Abstract
In this study, we investigated the effect of fluorine substitution on a previously reported diamine-based covalent organic framework (COF), designated as IPB-2H. A new fluorinated analogue namely IPB-2F2 was modeled and its adsorption and permeability characteristics for CO_2/N_2 gas mixtures were evaluated through computational analysis. Ab initio structural optimization results showed that the reduced pore size of IPB-2F2 compared to IPB-2H was attributed to the larger atomic size and higher electronegativity of fluorine compared to hydrogen atom. Molecular dynamics (MD) simulations demonstrated that IPB-2F2 exhibited lower permeation rates for CO_2 and N_2 than its non-fluorinated counterpart; indicating that fluorine atoms effectively reduced gas permeation. Adsorption isotherms revealed enhanced adsorption capacities for IPB-2F2, with increased CO_2 affinity resulting from strong van der Waals interactions. Selectivity analyses showed that IPB-2F2 preferentially absorbed CO_2 over N_2, with selectivity values consistently greater than 1. The enhanced gas uptake capacity and hydrophobicity of IPB-2F2 highlighted its potential for industrial applications as a post-combustion CO_2 capture material.

Keywords
Adsorption, Computational, CO_2 Capture, Permeability

Received: 19 July 2024, Accepted: 18 September 2024
https://doi.org/10.26554/sti.2025.10.1.18-26

1. INTRODUCTION

The need for effective CO_2 capture and storage (CCS) technologies has become increasingly critical in the face of escalating greenhouse gas emissions, mitigating environmental pollution and global climate change (Dziejarski et al., 2023; Ghiat and Al-Ansari, 2021). CCS involves capturing CO_2 emissions from industrial processes and power plants, transporting to storage sites, and sequestering to prevent the release of CO_2 into the atmosphere (Hanifa et al., 2023). A major obstacle in this field is the development of materials that selectively and efficiently captured CO_2 from gas mixtures, such as post-combustion flue gas, which predominantly consists of N_2 gas (Gambelli et al., 2021).

High regeneration costs, low selectivity, and stability issues are often encountered with current materials used for CO_2 capture, such as amine-based solvents and zeolites (Boer et al., 2023; Hanifa et al., 2023). Amine scrubbing, for instance, is widely used but is energy-intensive and suffers from degradation over time (Hanifa et al., 2023; Yoro et al., 2021). While zeolites often lack the necessary selectivity for CO_2 over N_2 molecules (Boer et al., 2023; Ganesan and Shaijumon, 2016). Metal-organic frameworks (MOFs) have shown promise due to their tunable pore structures and functionalization capabilities, yet their practical application is sometimes hindered by stability issues (Feng et al., 2020; Yuan et al., 2018). Covalent organic frameworks (COFs) have emerged as promising candidates in this regard due to their tunable porosity, high surface area, lightweight, and structural versatility (Liang et al., 2020; Zhao et al., 2018). These characteristics enable COFs to be designed with specific pore sizes and functional groups that enhance their attractive interactions towards CO_2 molecules, making them highly effective as selective adsorbents.

Fluorine substitution in adsorbing materials is a burgeoning area of research due to the potential enhancement in gas adsorption and separation properties. Fluorination has been shown to significantly alter the chemical and physical properties of materials, including increased hydrophobicity, enhanced thermal stability, and modified electronic properties (Liu et al., 2019). Fluorinated MOFs have been shown to enhance gas sorption due to the strong electrostatic interactions of certain gas molecules within the pore walls of porous materials

(Amooghin et al., 2022). Moghadam et al. (2017) have synthesized F-MOF-1 with the highest uptake of CO_2, which is 11.0 mol L^{-1} at 298 K and 55 bar and has strong hydrophobic properties. D'Amato et al. (2019), Chernikova et al. (2020), and Venturi et al. (2022) also report improved CO_2 capture performance and selectivity in fluorinated MOFs.

In our previously published study (Apriliyanto et al., 2020), we explored the adsorption sites and adsorption energies of CO_2 and N_2 molecules on 2D-COFs constructed from 1,3,5-tris(chloromethyl)benzene based building units and diamine based linkers (e.g. IPB-2H) using a combination of density functional theory (DFT) calculations and molecular dynamics (MD) simulations. Our findings demonstrated the competitive nature of these COFs with other 2D materials for carbon capture and separation applications, showcasing their efficient and rapid separation and adsorption capabilities. Based on our previous results, in this paper we focused on the computational analysis regarding CO_2/N_2 adsorption and permeability properties of fluorinated COFs. Specifically, we investigated the impact of substituting hydrogen with fluorine atoms in the benzene units of our previously reported COF (IPB-2H) producing a new fluorinated analogue structure, which designated as IPB-2F2 (Figure 1). This modification is expected to improve CO_2 adsorption capacity and selectivity, due to the distinctive electronic and steric effects introduced by the fluorine atoms. Our study employs advanced computational techniques to provide a detailed understanding of the intermolecular interactions and adsorption dynamics within these fluorinated COFs.

2. EXPERIMENTAL SECTION

2.1 Structural Modeling

The smallest unit cell of the IPB-2F2 COF determined via the topological approach was optimized for its structure and lattice parameters using ab initio methods employing the periodic DFT calculations using the Quantum ESPRESSO package (Giannozzi et al., 2017). The periodic model was constructed with initial supercell lattice parameters and sufficient vacuum space to prevent undesired interactions between layers along the z-axis. This supercell model adopted a hexagonal Bravais lattice configuration, comprising 78 atoms in total. Periodic DFT relaxations were conducted using the generalized gradient approximation (GGA) of Perdew-Burke-Ernzerhof (PBE) method. The projector augmented wave (PAW) pseudopotentials and an energy cutoff of 700 eV with $5 \times 5 \times 1$ Monkhorst-Pack k-points were implemented for the geometry optimizations (Bartolomei and Giorgi, 2016). After obtaining the optimum structure, the charge of each atom was calculated through single point DFT calculations using the B3LYP hybrid functional and RIJCOSX approximation with def2-TZVP basis. The partial atomic charge was then obtained through Hirshfeld analysis implemented in the ORCA quantum chemistry program (Neese et al., 2009).

2.2 Molecular Dynamics (MD) Simulations

In this study, MD simulations were conducted inside a $90.18 \times 78.09 \times 179.49$ $Å^3$ simulation box in the canonical ensemble (NVT) with periodic boundary conditions (PBC) by using the DL_POLY program (Smith et al., 2005). Simulations were performed at 353 K (a typical temperature of post-combustion flue gas) employing the Nose-Hoover thermostat with a 0.5 ps relaxation constant for systems composing of CO_2/N_2 gas mixture with ratio of 1:1 (Goethem et al., 2024). Pressure variation (1.00, 2.54, 3.18, 4.00, and 5.47 atm) was carried out by varying the amount of gas molecules using the Peng-Robinson equation of state. The IPB-2F2 and gas molecules were modelled as rigid bodies approach, thus only non-covalent interactions, i.e. electrostatic and non-electrostatic (van der Waals), were contributed to the total energies. A 15 Åcut-off distance was applied for both non-electrostatic and electrostatic interactions, in which the electrostatic contributions were computed via Ewald method and the non-electrostatic interactions via Improved Lennard-Jones (ILJ) potential (Apriliyanto et al., 2024). MD simulations lasted for 6 ns, including a 0.5 ns thermal equilibration, with a 1 fs time step. Trajectory data were then recorded every 2 ps and analyzed to determine permeation rate and adsorption isotherm.

3. RESULT AND DISCUSSION

3.1 IPB-2F2 COF Structure

COFs are nanoporous organic materials composed of periodically repeating units connected by covalent bonds, offering advantages such as low density, customizable pore size and structure, high thermal stability, and large surface area due to their light-element composition and strong covalent bonds (Feng et al., 2012; Huang et al., 2015). COFs have uniform pore sizes and can be tailored for various functions, enhancing their applicability in gas separation (Kumar et al., 2022; Liu et al., 2021). Herein, we proposed a novel fluorinated COF, denoted as IPB-2F2, that was newly designed from our previously reported IPB-2H structure (Apriliyanto et al., 2022) through the incorporation of fluorine atoms into the linker (Figure 2).

Structure optimization of IPB-2F2 was successfully performed using periodic DFT method within the PBE/PAW approach. The optimized structure of IPB-2F2 was evaluated by comparing it with the original COF structure (i.e. IPB-2H) to assess the impact of fluorine addition. IPB-2F2 exhibited a hexagonal lattice with optimized lattice parameters for a and b of 22.545 Å (Figure 2(a)), consistent with the hexagonal lattice vector angle of 120° and aligning with our previous results. In addition to the optimized lattice parameters, the optimized structural parameters in terms of bond radius and bond angle were benchmarked with other comparable structures. The optimized structural parameters are shown in the Table 1. Based on the results reported in Table 1, IPB-2F2 exhibits bond lengths and angles that are generally consistent with those of IPB-2H and some existing literatures. However, some deviations are present as consequences of strong fluorine electronegativity,

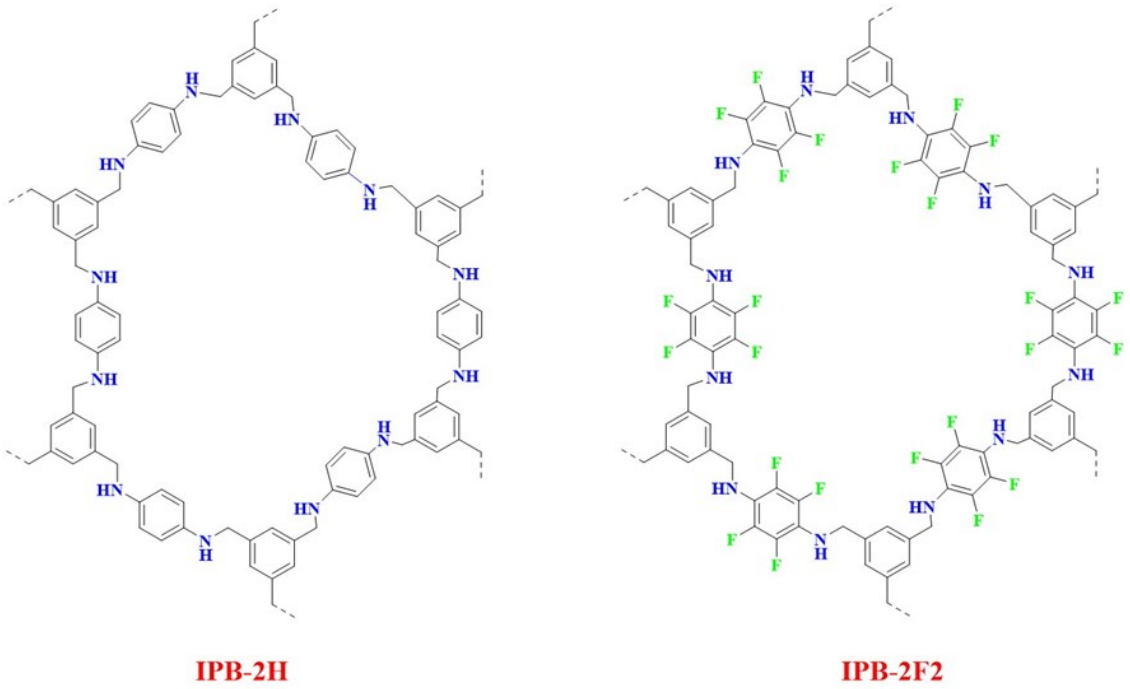

Figure 1. Two Dimensional (2D)-COFs Structures of IPB-2H (Apriliyanto et al., 2022) and IPB-2F2 (This Work)

which can redistribute electron density within molecules affecting their molecular geometry (Pilia et al., 2018).

Before conducting MD simulations, the partial charges of each atom in IPB-2F2 COF were determined to study the electrostatic interactions between CO_2/N_2 gas mixture and COF (Tong et al., 2016). Partial atomic charge parameters for a unit cell of IPB-2F2 were calculated using DFT method at B3LYP/def2-TZVP level, and these values were compared with those of IPB-2H. The pore size of IPB-2F2 COF shown in Figure 2(b) was estimated based on electron density method, yielded an effective pore size of 14.839 Å; which was smaller than 15.167 Åreported for IPB-2H. The reduction in pore size is attributed to the larger atomic size and higher electronegativity of fluorine atoms compared to hydrogen atoms, consistent with findings reported by Zhao et al. (2013) that fluorinated covalent triazine-based frameworks (CTFs) have smaller pore sizes (< 0.50 nm) compared to non-fluorinated CTFs.

3.2 Molecular Dynamics (MD) Simulations Results

MD simulations were conducted to investigate the interactions between the IPB-2F2 membrane and CO_2/N_2 gas mixture at 353 K, simulating post-combustion conditions. The optimized IPB-2F2 membrane with a size of 90.18×78.09 Å^2 was placed in the center of the simulation box (Figure 3), where CO_2 andN_2 molecules were randomly placed according to predetermined pressure variations. In this study, we consider CO_2/N_2 mixture to model flue gas where nitrogen gas always limits the CO_2 uptake capacity of a material. Moreover, we choose the gas ratio to be 1:1 to study the competitive intermolecular interactions between CO_2-COF and N_2-COF as an equal fraction. Therefore, the gas uptake capacity and selectivity of the materials can be measured fairly without domination of a certain gas molecule.

The IPB-2F2 as well as the CO_2 and N_2 gas molecules were treated as rigid structures during the MD simulations. At the time of simulations, thermal equilibration was first carried out for 0.5 ns followed by simulation and calculation of intermolecular interactions for 5.5 ns. Trajectory data and simulation results were compiled every 2 ps, so that about 3000 frames were obtained from each performed simulation. Several parameters were evaluated to assess the performance of the IPB-2F2 membrane compared to IPB-2H; including permeability, adsorption capacity, and selectivity. The permeance value for each gas was obtained from the slope of the permeation rate line against pressure (Figure 4, left panel). At identical pressures, the permeation rates of CO_2 and N_2 molecules for IPB-2F2 are lower than those reported for IPB-2H. This indicates that the addition of fluorine atoms can restrain the permeation rate of gas molecules, particularlyCO_2. Yan et al. (2019) suggest that the high electronegativity of fluorine atoms enhances the affinity forCO_2 molecules, thereby increasingCO_2 adsorption and decreasingCO_2 permeation for the fluorinated COFs membrane.

Figure 4 (left panel) shows thatCO_2 permeance value is higher than N_2 molecules. This is due to the attraction of IPB-2F2 towardsCO_2 gas molecules is stronger than N_2. Figure 4 right panel, illustrates the adsorption isotherm curves, showing the average adsorbed gas per surface area unit of membrane against the applied pressure for both IPB-2F2 and IPB-2H COFs. The stronger affinity for CO_2 molecules is also

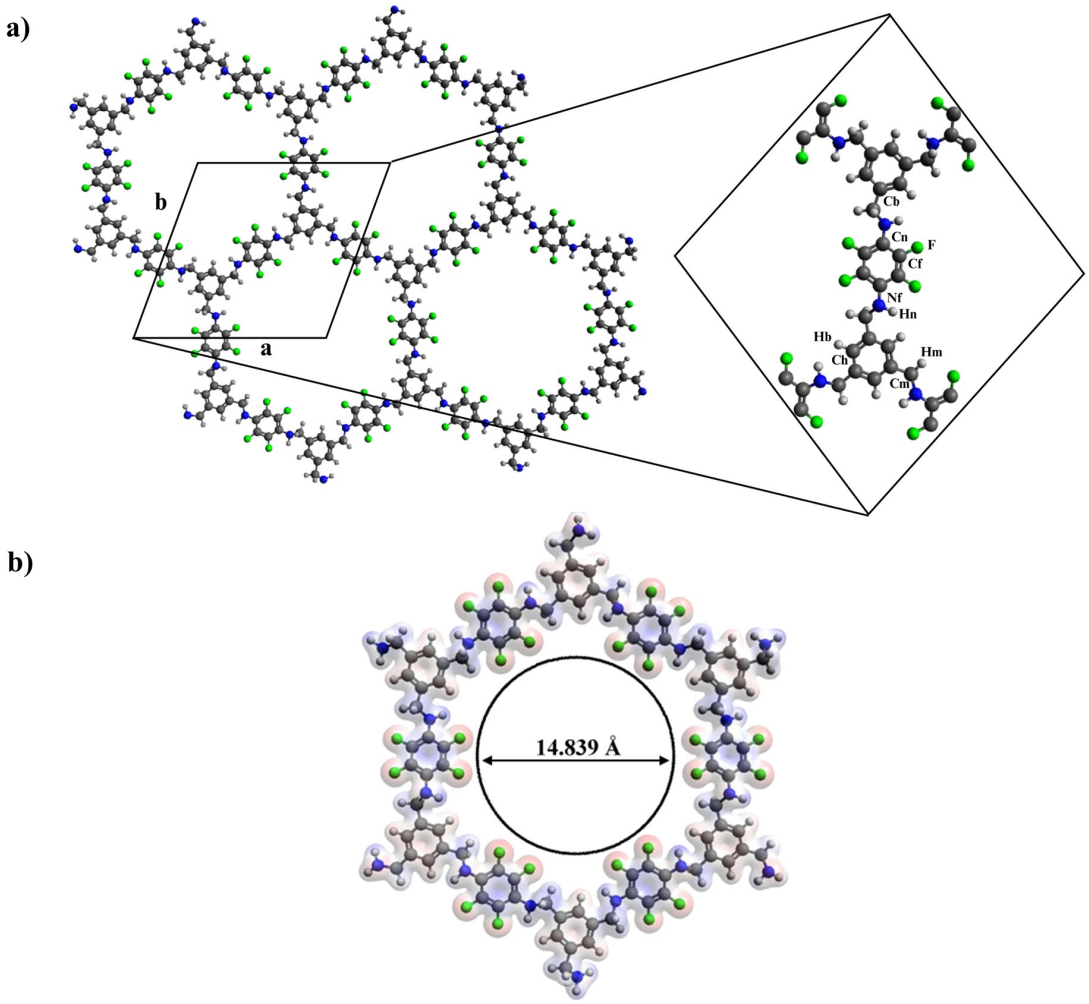

Figure 2. IPB-2F2 Represented by Its Hexagonal Lattice Structure Used in The Periodic DFT Relaxations Along with Its Atomic Labelling (a). A Unit Pore of IPB-2F2 Represented by The Electron Density (Iso-Value = 0.02 E $Bohr^{-3}$) (b)

manifested in the corresponding adsorption isotherm. The relationship between the amount of adsorbed gas on the membrane surface and the gas pressure at a constant temperature, the adsorption isotherm, can be used to explain adsorption phenomenon (Lee et al., 2021). IPB-2F2 exhibited a higher adsorption isotherm curve for CO_2 and N_2 gases than IPB-2H, indicating that IPB-2F2 can adsorb more gas molecules. The linear relationship between pressure and the amount of gas adsorbed further confirms the enhanced adsorption capacity of IPB-2F2. We also found that CO_2 gas tended to be adsorbed near the fluorine atoms of the IPB-2F2 membrane, as the fluorine atoms continuously attracted CO_2 molecules. As illustrated in Figure 5, the gas density plotted along the z-axis demonstrated that the amount of adsorbed CO_2 increases proportionally with pressure. Indeed, higher pressures lead to a greater probability of CO_2 adsorption on the IPB-2F2 membrane.

The gas adsorption on the IPB-2F2 surface is driven by intermolecular interactions comprising both electrostatic and van der Waals contributions. Table 2 presents the van der Waals and Coulombic (electrostatic) energy components obtained from molecular dynamics (MD) simulations, clearly demonstrating that electrostatic interactions dominate the overall energy profile. This dominance is expected due to the long-range nature of Coulombic interactions, emphasizing the importance of accurately determining partial atomic charges. In contrast, van der Waals interactions contribute minimally to the total interaction energy. However, upon closer inspection of Table 2, the observed differences between systems at varying pressures are primarily attributed to van der Waals forces. While Coulombic energies remain consistent across different pressures, van der Waals interactions differentiate the systems, indicating that increased pressure enhances CO_2 adsorption on IPB-2F2 due to the influence of van der Waals forces (Figures 4 and 5). Consequently, the application of an improved Lennard-Jones potential is critical to accurately model these

Table 1. The Optimized Structural Parameters of IPB-2F2 in Terms of Bond Radius (Å) and Bond Angle (°) in Comparison with Other Structures in Existing Literatures

Parameters	IPB-2F2	IPB-2H[1]	CTF-0[2]	Benzoimidazole-Based Hydrazones[3]	BND-TFB[4]
r Cf-F	1.36	-	-	1.35	-
r Cn-N	1.40	1.40	-	-	-
r Cf-Cn (cyclic)	1.40	1.41	1.40	1.40	-
r Cn-Cf (cyclic)	1.41	1.41	1.40	1.40	-
r Cf-Cf	1.39	1.41	1.40	1.40	-
r Cb-Cm ($sp^2 - sp^3$)	1.51	1.51	1.48	1.51	-
r Cb-Ch (cyclic)	1.40	1.41	1.40	1.40	-
r Cm-Nf	1.47	1.45	-	-	-
∠Cb-Ch-Cb	121.30	121.40	-	-	120.70
∠Ch-Cb-Ch	118.80	118.70	-	-	119.30
∠Cb-Cm-Nf	114.10	114.50	-	-	-
∠Ch-Cb-Cm	122.90	123.90	-	-	121.40
∠Cb-Ch-Hb	120.60	121.00	-	-	120.20
∠Cm-Nf-Hn	112.70	114.10	-	-	-
∠Cm-Nf-Cn	117.10	119.90	-	-	-
∠Cn-Cf-Cf	122.20	121.10	-	-	120.50
∠Cf-Cn-Cf	115.40	117.50	-	-	118.70
∠Cn-Cf-F	118.40	-	-	-	-

Source: [1]Apriliyanto et al. (2020), [2]Wang et al. (2016), [3]Rafiq et al. (2019), [4]Vitaku and Dichtel (2017)

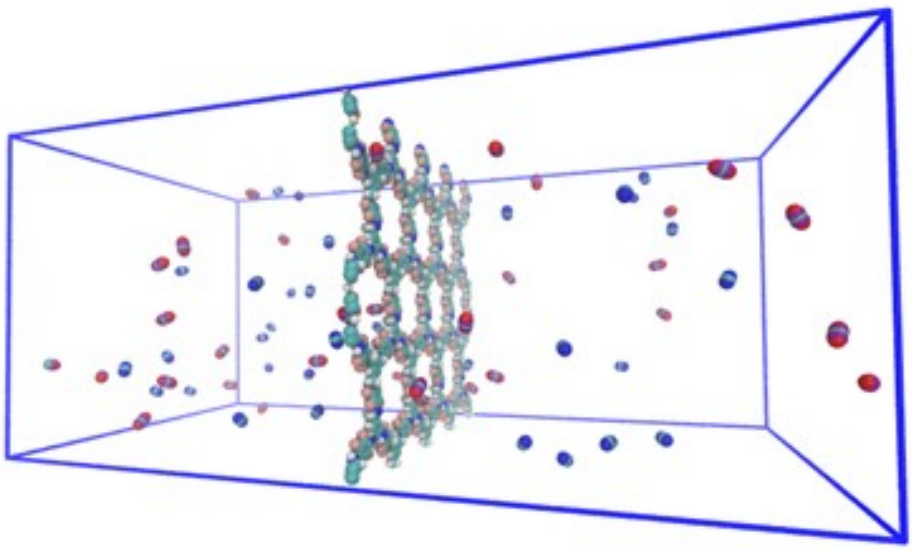

Figure 3. Snapshot of The Simulation Box at P = 2.54 atm. N_2 Molecules are Colored Blue, While CO_2 Molecules are Colored Cyan and Red

short-range interactions compared to the standard Lennard-Jones potential.

Furthermore, the diffusion and adsorption coefficients for IPB-2F2 were compared with those of IPB-2H (Table 3). The diffusion coefficient, defined as the rate of gas movement through the membrane, was lower for IPB-2F2 under the same pressure conditions suggesting that the stronger attraction due to fluorine addition inhibited gas diffusion. Moreover, the diffusion coefficient decreased with increasing pressure, indicating that a greater number of gas molecules could impede the movement of other molecules through the membrane. Conversely, the adsorption coefficient, derived from the slope of the adsorption isotherm curve, was higher for IPB-2F2 than for IPB-2H. This suggests that IPB-2F2 absorbs more gas molecules, at-

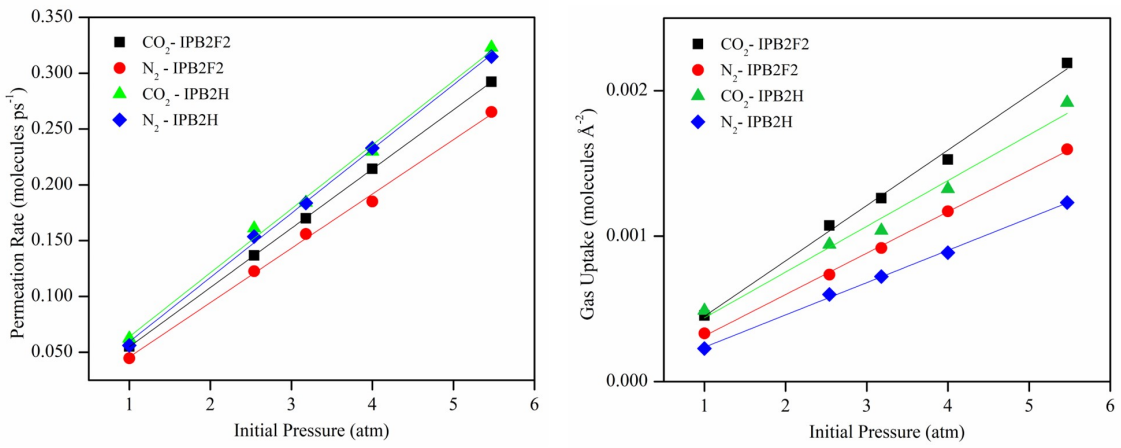

Figure 4. Permeation Rate as a Function of Initial Pressure (Left Panel) and Adsorption Isotherms (Right Panel) of IPB-2F2 and IPB-2H at 353 K

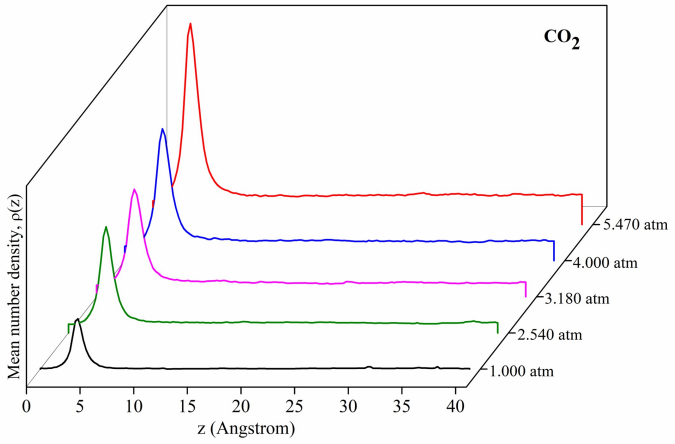

Figure 5. The z-density Profiles of CO_2 Adsorption from the IPB-2F2 Surface

tributed to weak intermolecular forces such as van der Waals interactions between fluorine atoms and CO_2 molecules. It was reported that the C−F bond's longer length (0.1332 nm) and greater strength (111 kcal mol^{-1}) compared to C−H bonds, along with its strong polarity, further enhanced CO_2 adsorption (Yu et al., 2012).

Adsorption selectivity parameter was calculated based on Equation (1). The selectivity results showed that the CO_2/N_2 gas selectivity of IPB-2F2 was not significantly different from that of IPB-2H (Table 4). This indicates that the IPB-2F2 membrane absorbs both CO_2 and N_2 strongly. The adsorption isotherm curve also showed an increase in the number of adsorbed gas molecules for both gases. This finding contrasts with the work of Zhao et al. (2013), who reported increased CO_2 selectivity in fluorinated Covalent Triazine-based Frameworks (F-CTF) due to multilayer membrane structures. Tong et al. (2016) also noted that overlapped CTF-1 membranes exhibit

Table 2. The van der Waals and Coulomb Energies Measured During the MD Simulations

P (atm)	van der Waals (kcal mol^{-1})	Coulomb (kcal mol^{-1})
1.000	-4.870 ± 4.327	-206.460 ± 0.303
2.540	-9.755 ± 3.654	-206.590 ± 0.456
3.180	-10.861 ± 3.553	-206.640 ± 0.496
4.000	-13.316 ± 4.156	-206.690 ± 0.549
5.470	-20.010 ± 4.805	-206.950 ± 0.706

higher selectivity than single-layer membranes, a phenomenon similarly reported Apriliyanto et al. (2022) for graphtriyne membranes with trilayer structures showing the highest selectivity. It is important to note that in this study, IPB-2F2 was examined in its monolayer form, and different adsorption behaviors may be observed with multilayer membranes.

Despite the adsorption selectivity of IPB-2F2 is lower than IPB-2H, the selectivity value of IPB-2F2 remained greater than 1, indicating that the membrane is selective for CO_2 with CO_2 molecules more readily adsorbed on the membrane surface than N_2. These selectivity results are comparable with other 2D materials in its monolayer form reported in Table 4. The IPB-2F2 is even better than those reported by Tong et al. (2016) and Goethem et al. (2024), where the CTF-1 membrane and NPC film are not selective by only showing a selectivity of 0.89 and 0.90, respectively. Additionally, structural modification by adding fluorine atoms can make the membrane more hydrophobic, suggesting its potential application in industrial flue gases where it may resist the influence of water vapor Ozdemir et al. (2019).

$$S_{ads}^{CO_2/N_2} = \frac{n_{CO_2}ads}{n_{CO_2}free} \times \frac{n_{N_2}ads}{n_{N_2}free} \quad (1)$$

Table 3. Diffusion and Adsorption Coefficients for CO_2/N_2 Mixture Systems at 353 K

Coefficient	P (atm)	IPB-2F2		IPB-2H[1]	
		CO_2	N_2	CO_2	N_2
Diffusion ($\times 10^{-6}$ m^2 s^{-1})	1.000	1.857	2.077	2.162	4.236
	2.540	2.833	2.792	3.030	3.592
	3.180	1.814	1.561	2.003	3.155
	4.000	1.625	2.010	1.962	2.569
	5.470	1.677	2.583	1.781	2.233
Adsorption (molecule Å^{-}2 atm^{-1})		3.81 × 10–4	2.85×10^{-4}	3.14×10^{-4}	2.22×10^{-4}

Source: [1]Apriliyanto et al. (2020)

Table 4. Comparison of CO_2/N_2 Selectivity Between IPB-2F2 and Other 2D Materials in Existing Literatures

Materials	System's condition	Selectivity	Ref.
IPB-2F2	1.00; 2.54; 3.18; 4.00; 5.47 atm & 353 K	1.48; 1.58; 1.46; 1.37; 1.46	This work
IPB-2H	1.00; 2.54; 3.18; 4.00; 5.47 atm & 353 K	2.53; 1.71; 1.52; 1.59; 1.67	Apriliyanto et al. (2020)
Nanoporous carbon (NPC) film	1.97 atm & 308 K	0.90	Goethem et al. (2024)
g-C10N9 membrane	298 K (pressure not specified)	1.00	Chang et al. (2018)
Bilayer graphene oxide (GO) sheets (W2, D = 9 Å)	127.71 atm & 298 K	1.00	Wang et al. (2017)
Graphdiyne-like monolayers (GDY_H; GDY_F)	2.96 atm & 298 K	1.10; 1.70	Zhao et al. (2017)
Valent triazine-based frameworks (CTF-1)	9.87 atm & 300 K	0.89	Tong et al. (2016)
Squaraine-bridged COFs (SQ-COPs-2/3)	< 9.87 atm & 298 K	1.50	Huang and Cao (2016)
Graphene oxide (GO) membrane (8.3 Åspacing)	298 K (pressure not specified)	1.00-1.30	Li et al. (2016)
Fluorine-modified porous graphene	300 K (pressure not specified)	1.69	Wu et al. (2014)

4. CONCLUSIONS

The effects of fluorine substitution in diamine COF (IPB-2F2) performance on CO_2/N_2 adsorption and separation have been investigated through computational analysis by means of DFT calculations and MD simulations. Structural optimizations results revealed a reduced pore size for IPB-2F2 in comparison with IPB-2H due to fluorine's large atomic size and high electronegativity. MD simulations showed that IPB-2F2 had lower CO_2 and N_2 permeation rates than IPB-2H, indicating that fluorine atoms reduced gas permeation. Adsorption isotherms demonstrated that fluorine substitution enhanced gas uptake capacities of COF. From an energetical point of view, gas adsorption on the surface of COFs was mainly governed by the van der Waals interactions. Therefore, substituting hydrogen with fluorine atoms that had higher polarizability increased gas adsorption by magnifying the dispersion forces (a main component of van der Waals forces). Selectivity analysis indicated that IPB-2F2 preferentially adsorbs CO_2 over N_2, with adsorption selectivity values consistently greater than 1. Finally, the enhanced hydrophobicity of IPB-2F2 suggests suitability for industrial applications as CO_2 capture material, where the post-combustion flue gas contains water vapor.

5. ACKNOWLEDGMENT

We would like to express our gratitude for the research funding provided by the Indonesian Endowment Fund for Education (LPDP) through the Equity Program (DAPT), specifically under the national research collaboration scheme/Riset Kolaborasi Nasional (Ri-Na) under contract number 525/IT3.D10/PT .01.03/P/B/2023.

REFERENCES

Amooghin, A. E., H. Sanaeepur, R. Luque, H. Garcia, and B. Chen (2022). Fluorinated Metal–Organic Frameworks for Gas Separation. *Chemical Society Reviews*, **51**(17); 7427–7508

Apriliyanto, Y. B., N. Darmawan, N. Faginas-Lago, and A. Lombardi (2020). Two-Dimensional Diamine-Linked Covalent Organic Frameworks for CO_2/N_2 Capture and Separation: Theoretical Modeling and Simulations. *Physical Chemistry Chemical Physics*, **22**(44); 25918–25929

Apriliyanto, Y. B., N. Faginas-Lago, S. Evangelisti, M. Bartolomei, T. Leininger, F. Pirani, L. Pacifici, and A. Lombardi (2022). Multilayer Graphtriyne Membranes for Separation and Storage of CO_2: Molecular Dynamics Simulations of Post-Combustion Model Mixtures. *Molecules*, **27**(18); 5958

Apriliyanto, Y. B., A. Lombardi, L. Mancini, F. Pirani, and N. Faginas-Lago (2024). Revisiting Numerical Solutions of Weakly Bound Noble Gases' Vibrational Energy Levels Modeled by the Improved Lennard-Jones Potential. *ChemPhysChem*, **June**; e202400223

Bartolomei, M. and G. Giorgi (2016). A Novel Nanoporous Graphite Based on Graphynes: First-Principles Structure and Carbon Dioxide Preferential Physisorption. *ACS Applied Materials & Interfaces*, **8**(41); 27996–28003

Boer, D. G., J. Langerak, and P. P. Pescarmona (2023). Zeolites as Selective Adsorbents for CO_2 Separation. *ACS Applied Energy Materials*, **6**(5); 2634–2656

Chang, X., L. Zhu, Q. Xue, X. Li, T. Guo, X. Li, and M. Ma (2018). Charge Controlled Switchable CO_2/N_2 Separation for g-C10N9 Membrane: Insights from Molecular Dynamics Simulations. *Journal of CO_2 Utilization*, **26**; 294–301

Chernikova, V., O. Shekhah, Y. Belmabkhout, and M. Eddaoudi (2020). Nanoporous Fluorinated Metal–Organic Framework-Based Membranes for CO_2 Capture. *ACS Applied Nano Materials*, **3**(7); 6432–6439

Dziejarski, B., R. Krzyzynska, and K. Andersson (2023). Current Status of Carbon Capture, Utilization, and Storage Technologies in the Global Economy: A Survey of Technical Assessment. *Fuel*, **342**; 127776

D'Amato, R., A. Donnadio, M. Carta, C. Sangregorio, D. Tiana, R. Vivani, M. Taddei, and F. Costantino (2019). Water-Based Synthesis and Enhanced CO_2 Capture Performance of Perfluorinated Cerium-Based Metal–Organic Frameworks with UiO-66 and MIL-140 Topology. *ACS Sustainable Chemistry & Engineering*, **7**(1); 394–402

Feng, L., K.-Y. Wang, G. S. Day, M. R. Ryder, and H.-C. Zhou (2020). Destruction of Metal–Organic Frameworks: Positive and Negative Aspects of Stability and Lability. *Chemical Reviews*, **120**(23); 13087–13133

Feng, X., X. Ding, and D. Jiang (2012). Covalent Organic Frameworks. *Chemical Society Reviews*, **41**(18); 6010

Gambelli, A. M., A. Presciutti, and F. Rossi (2021). Review on the Characteristics and Advantages Related to the Use of Flue-Gas as CO_2/N_2 Mixture for Gas Hydrate Production. *Fluid Phase Equilibria*, **541**; 113077

Ganesan, A. and M. M. Shaijumon (2016). Activated Graphene-Derived Porous Carbon with Exceptional Gas Adsorption Properties. *Microporous and Mesoporous Materials*, **220**; 21–27

Ghiat, I. and T. Al-Ansari (2021). A Review of Carbon Capture and Utilisation as a CO_2 Abatement Opportunity within the EWF Nexus. *Journal of CO_2 Utilization*, **45**; 101432

Giannozzi, P., O. Andreussi, T. Brumme, O. Bunau, M. Buongiorno Nardelli, M. Calandra, R. Car, C. Cavazzoni, D. Ceresoli, M. Cococcioni, N. Colonna, I. Carnimeo, A. Dal Corso, S. de Gironcoli, P. Delugas, R. A. DiStasio, A. Ferretti, A. Floris, G. Fratesi, and S. Baroni (2017). Advanced Capabilities for Materials Modelling with Quantum ESPRESSO. *Journal of Physics: Condensed Matter*, **29**(46); 465901

Goethem, C. V., Y. Shen, H. Y. Chi, M. Mensi, K. Zhao, A. Nijmeijer, J. P., and K. V. Agrawal (2024). Advancing Molecular Sieving via Å-Scale Pore Tuning in Bottom-Up Graphene Synthesis. *ACS Nano*, **18**(7); 5730–5740

Hanifa, M., R. Agarwal, U. Sharma, P. C. Thapliyal, and L. P. Singh (2023). A Review on CO_2 Capture and Sequestration in the Construction Industry: Emerging Approaches and Commercialised Technologies. *Journal of CO_2 Utilization*, **67**; 102292

Huang, L. and G. Cao (2016). 2D Squaraine-Bridged Covalent Organic Polymers with Promising CO_2 Storage and Separation Properties. *ChemistrySelect*, **1**(3); 533–538

Huang, L., M. Zhang, C. Li, and G. Shi (2015). Graphene-Based Membranes for Molecular Separation. *The Journal of Physical Chemistry Letters*, **6**(14); 2806–2815

Kumar, S., M. A. Abdulhamid, A. D. Dinga Wonanke, M. A. Addicoat, and G. Szekely (2022). Norbornane-Based Covalent Organic Frameworks for Gas Separation. *Nanoscale*, **14**(6); 2475–2481

Lee, T. H., F. Moghadam, J. G. Jung, Y. J. Kim, J. S. Roh, S. Y. Yoo, B. K. Lee, J. H. Kim, I. Pinnau, and H. B. Park (2021). In Situ Derived Hybrid Carbon Molecular Sieve Membranes with Tailored Ultramicroporosity for Efficient Gas Separation. *Small*, **17**(47)

Li, W., X. Zheng, Z. Dong, C. Li, W. Wang, Y. Yan, and J. Zhang (2016). Molecular Dynamics Simulations of CO_2/N_2 Separation Through Two-Dimensional Graphene Oxide Membranes. *The Journal of Physical Chemistry C*, **120**(45); 26061–26066

Liang, R., S. Jiang, R.-H. A, and X. Zhao (2020). Two-Dimensional Covalent Organic Frameworks with Hierarchical Porosity. *Chemical Society Reviews*, **49**(12); 3920–3951

Liu, R., K. T. Tan, Y. Gong, Y. Chen, Z. Li, S. Xie, T. He, Z. Lu, H. Yang, and D. Jiang (2021). Covalent Organic Frameworks: An Ideal Platform for Designing Ordered Materials and Advanced Applications. *Chemical Society Reviews*, **50**(1); 120–242

Liu, Y., L. Jiang, H. Wang, H. Wang, W. Jiao, G. Chen, P. Zhang, D. Hui, and X. Jian (2019). A Brief Review for

Fluorinated Carbon: Synthesis, Properties and Applications. *Nanotechnology Reviews*, **8**(1); 573–586

Moghadam, P. Z., J. F. Ivy, R. K. Arvapally, A. M. dos Santos, J. C. Pearson, L. Zhang, E. Tylianakis, P. Ghosh, I. W. H. Oswald, U. Kaipa, X. Wang, A. K. Wilson, R. Q. Snurr, and M. A. Omary (2017). Adsorption and Molecular Siting of CO_2, Water, and Other Gases in the Superhydrophobic, Flexible Pores of FMOF-1 from Experiment and Simulation. *Chemical Science*, **8**(5); 3989–4000

Neese, F., F. Wennmohs, A. Hansen, and U. Becker (2009). Efficient, Approximate and Parallel Hartree-Fock and Hybrid DFT Calculations. A 'Chain-of-Spheres' Algorithm for the Hartree-Fock Exchange. *Chemical Physics*, **356**(1–3); 98–109

Ozdemir, J., I. Mosleh, M. Abolhassani, L. F. Greenlee, R. R. Beitle, and M. H. Beyzavi (2019). Covalent Organic Frameworks for the Capture, Fixation, or Reduction of CO2. *Frontiers in Energy Research*, **7**; 77

Pilia, L., Y. Shuku, S. Dalgleish, K. Awaga, and N. Robertson (2018). Structural and Electronic Effects Due to Fluorine Atoms on Dibenzotetraaza-Annulenes Complexes. *ACS Omega*, **3**(8); 10074–10083

Rafiq, M., M. Khalid, M. N. Tahir, M. U. Ahmad, M. U. Khan, M. M. Naseer, A. A. C. Braga, S. Muhammad, and Z. Shafiq (2019). Synthesis, XRD, Spectral (IR, UV-Vis, NMR) Characterization and Quantum Chemical Exploration of Benzoimidazole-Based Hydrazones: A Synergistic Experimental-Computational Analysis. *Applied Organometallic Chemistry*, **33**(11); e5182

Smith, W., I. T. Todorov, and M. Leslie (2005). The DL_POLY Molecular Dynamics Package. *Zeitschrift Für Kristallographie - Crystalline Materials*, **220**(5–6); 563–566

Tong, M., Q. Yang, Q. Ma, D. Liu, and C. Zhong (2016). Few-Layered Ultrathin Covalent Organic Framework Membranes for Gas Separation: A Computational Study. *Journal of Materials Chemistry A*, **4**(1); 124–131

Venturi, D. M., M. S. Notari, R. Bondi, E. Mosconi, W. Kaiser, G. Mercuri, G. Giambastiani, A. Rossin, M. Taddei, and F. Costantino (2022). Increased CO_2 Affinity and Adsorption Selectivity in MOF-801 Fluorinated Analogues. *ACS Applied Materials & Interfaces*, **14**(36); 40801–40811

Vitaku, E. and W. R. Dichtel (2017). Synthesis of 2D Imine-Linked Covalent Organic Frameworks Through Formal Transimination Reactions. *Journal of the American Chemical Society*, **139**(37); 12911–12914

Wang, P., W. Li, C. Du, X. Zheng, X. Sun, Y. Yan, and J. Zhang (2017). CO_2/N_2 Separation via Multilayer Nanoslit Graphene Oxide Membranes: Molecular Dynamics Simulation Study. *Computational Materials Science*, **140**; 284–289

Wang, Y., J. Li, Q. Yang, and C. Zhong (2016). Two-Dimensional Covalent Triazine Framework Membrane for Helium Separation and Hydrogen Purification. *ACS Applied Materials & Interfaces*, **8**(13); 8694–8701

Wu, T., Q. Xue, C. Ling, M. Shan, Z. Liu, Y. Tao, and X. Li (2014). Fluorine-Modified Porous Graphene as Membrane for CO_2/N_2 Separation: Molecular Dynamic and First-Principles Simulations. *The Journal of Physical Chemistry C*, **118**(14); 7369–7376

Yan, T., Y. Lan, M. Tong, and C. Zhong (2019). Screening and Design of Covalent Organic Framework Membranes for CO_2/CH_4 Separation. *ACS Sustainable Chemistry & Engineering*, **7**(1); 1220–1227

Yoro, K. O., M. O. Daramola, P. T. Sekoai, E. K. Armah, and U. N. Wilson (2021). Advances and Emerging Techniques for Energy Recovery During Absorptive CO_2 Capture: A Review of Process and Non-Process Integration-Based Strategies. *Renewable and Sustainable Energy Reviews*, **147**; 111241

Yu, H., S. Cho, B. Chol, K. Bok, and Y. Lee (2012). Effects of Fluorination on Carbon Molecular Sieves for CH_4/CO_2 Gas Separation Behavior. *International Journal of Greenhouse Gas Control*, **10**; 278–284

Yuan, S., L. Feng, K. Wang, J. Pang, M. Bosch, C. Lollar, Y. Sun, J. Qin, X. Yang, P. Zhang, Q. Wang, L. Zou, Y. Zhang, L. Zhang, Y. Fang, J. Li, and H. Zhou (2018). Stable Metal–Organic Frameworks: Design, Synthesis, and Applications. *Advanced Materials*, **30**(37); 1–35

Zhao, F., H. Liu, S. D. R. Mathe, A. Dong, and J. Zhang (2018). Covalent Organic Frameworks: From Materials Design to Biomedical Application. *Nanomaterials*, **8**(1)

Zhao, L., P. Sang, S. Guo, X. Liu, J. Li, H. Zhu, and W. Guo (2017). Promising Monolayer Membranes for $CO_2/N_2/CH_4$ Separation: Graphdiynes Modified Respectively with Hydrogen, Fluorine, and Oxygen Atoms. *Applied Surface Science*, **405**; 455–464

Zhao, Y., K. X. Yao, B. Teng, T. Zhang, and Y. Han (2013). A Perfluorinated Covalent Triazine-Based Framework for Highly Selective and Water-Tolerant CO_2 Capture. *Energy & Environmental Science*, **6**(12); 3684

